ADVANCES IN ATMOSPHERIC SCIENCES, VOL. 32, OCTOBER 2015, 1407–1418

Sensitivity of Tropical Cyclone Intensification to Inner-Core Structure

GE Xuyang*[1,2], XU Wei[1], and ZHOU Shunwu[1]

[1] *Key laboratory of Meteorological Disaster, Collaborative Innovation Center on Forecast and Evaluation of Meteorological Disasters, Nanjing University of Information Science & Technology, Nanjing* 210044

[2] *State Key Laboratory of Severe Weather, Chinese Academy of Meteorological Sciences, Beijing* 100081

(Received 30 December 2014; revised 8 March 2015; accepted 26 March 2015)

ABSTRACT

In this study, the dependence of tropical cyclone (TC) development on the inner-core structure of the parent vortex is examined using a pair of idealized numerical simulations. It is found that the radial profile of inner-core relative vorticity may have a great impact on its subsequent development. For a system with a larger inner-core relative vorticity/inertial stability, the conversion ratio of the diabatic heating to kinetic energy is greater. Furthermore, the behavior of the convective vorticity eddies is likely modulated by the system-scale circulation. For a parent vortex with a relatively higher inner-core vorticity and larger negative radial vorticity gradient, convective eddy formation and radially inward propagation is promoted through vorticity segregation. This provides a greater potential for these small-scale convective cells to self-organize into a mesoscale inner-core structure in the TC. In turn, convectively induced diabatic heating that is close to the center, along with higher inertial stability, efficiently enhances system-scale secondary circulation. This study provides a solid basis for further research into how the initial structure of a TC influences storm dynamics and thermodynamics.

Key words: tropical cyclone, intensification, inner-core structure

Citation: Ge, X. Y., W. Xu, and S. W. Zhou, 2015: Sensitivity of tropical cyclone intensification to inner-core structure. *Adv. Atmos. Sci.*, **32**(10), 1407–1418, doi: 10.1007/s00376-015-4286-5.

1. Introduction

Although forecasts of hurricane tracks have steadily improved during the past few decades, tropical cyclone (TC) genesis and intensity forecasts remain unsatisfactory (Elsberry, 2005). In terms of TC genesis, numerous studies (Hendricks et al., 2004; Montgomery et al., 2006; Tory et al., 2006; Nolan, 2007; Ge et al., 2013a; Liang et al., 2014) suggest that the merger of multiple smaller vortices into a mesoscale inner-core structure is a key step. However, details on how the parent vortex or incipient disturbance affects this merger process have not been well studied. In operational forecasting, parent vortex structures can significantly affect the behavior of hurricane intensity (Kurihara et al., 1993; Leslie and Holland, 1995; Willoughby and Black, 1996). Because of the paucity of observations, the so-called bogussing vortex technique is often adopted to improve storm representation in many operational centers (Kurihara et al., 1993; Liu et al., 2006; Hendricks et al., 2011). Generally, this method is simply based on traditional parameters such as maximum wind speed (Vmax), the radius of maximum winds (RMW), and minimum sea-level pressure (MSLP). Even when the quantities of such parameters are similar, the storm structure could be distinct if different wind-pressure relationships are applied.

In terms of TC intensity change, previous studies have primarily focused on the large-scale environmental control (Wang and Zhou, 2008; Wu et al., 2011; Ge et al., 2013b). Xu and Wang (2010) investigated the sensitivity of TC development to the initial storm size and found that TC intensification and structure are sensitive to the outer circulation (i.e., the wind profile beyond the RMW). Recently, Rogers et al. (2013) found that one of the key inner-core structural differences between intensifying and steady-state TCs is the radial location of convective bursts. Specifically, for intensifying TCs, it is preferentially located inside the RMW, whereas for steady-state TCs the bursts are located outside the RMW. Observational and numerical studies suggest that small-scale convective systems play an important role in TC genesis (Hendricks et al., 2004; Montgomery et al., 2006). These studies strongly support the idea that the merger of multiple smaller vortices into a larger "parent" vortex is a key part of the genesis process. That is, interactions of different-scale systems in vorticity-rich areas act as important contributing mechanisms for TC genesis or development. However, the relationship between TC inner-core structure and the behavior of the convective system are not well understood. Hence, in this study, we attempt to scrutinize how the initial parent vortex modulates the embedded small-scale convective cells

* Corresponding author: GE Xuyang
Email: xuyang@nuist.edu.cn

and thus influences its subsequent evolution. In other words, the primary goal here is to illustrate the sensitivity of TC development to its initial inner-core structure.

The paper is organized as follows: The model and experimental design are briefly introduced in section 2. The preliminary results are presented in section 3. Finally, in section 4, a short summary and discussion are given.

2. Model and experimental design

In this study, version 3.3.1 of the Advanced Research Weather Research and Forecasting model (WRF_ARW) is used. This model is triple-nested with two-way interaction. The mesh sizes in the three domains are 241×241, with horizontal dimensions of 27, 9 and 3 km, respectively. There are 28 vertical levels. The microphysics scheme (Lin et al., 1983) is applied in all meshes. The model is initialized with a weak axisymmetric cyclonic vortex on an f-plane located at 15°N in a quiescent environment with a constant SST of 29°C. The environmental sounding is based on mean tropical sounding (Jordan, 1958). To investigate the sensitivity of TC intensification to inner-core structure, two idealized vortices are designed. Figures 1a and b display the vertical–radial profiles of tangential wind and associated temperature anomalies. Specifically, the tangential wind profiles are specified as follows:

$$\text{CTL}: V_t = V_m \times \left(\frac{r}{r_m}\right) \times \left[\exp\left(1-\frac{r}{r_m}\right) - \left|\frac{r-r_m}{r_0-r_m}\right| \times \exp\left(1-\frac{r_0}{r_m}\right)\right]; \quad (1)$$

$$\text{RANK}: V_t = \frac{V_m}{r_m} \times r\,, r \leqslant r_m\,. \quad (2)$$

Beyond the RMW, the tangential winds in both cases are the same as defined by Eq. (1), in which V_m is the maximum wind speed, r_m is the RMW, r is the radius, and r_0 is set to

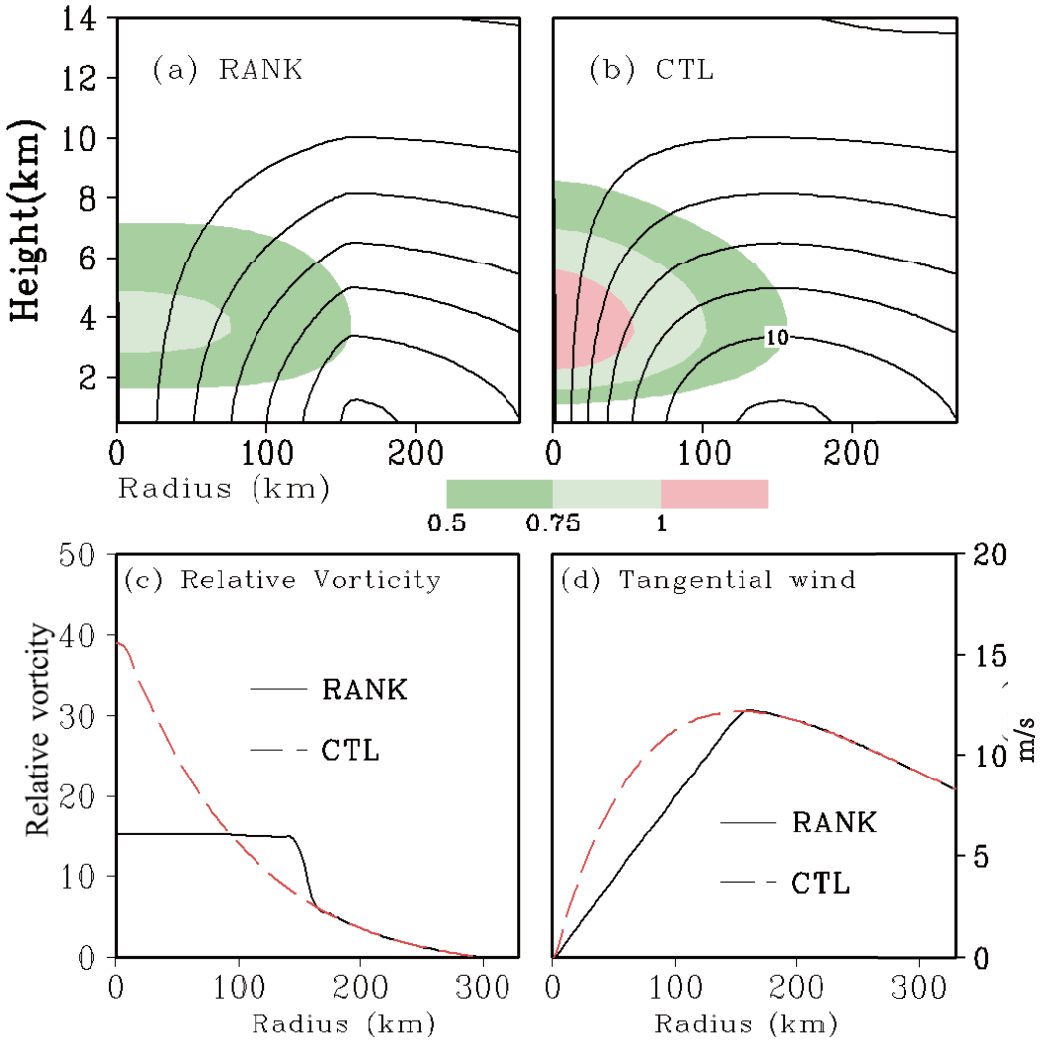

Fig. 1. Top panels: vertical–radial profiles of tangential wind (contours; units: m s^{-1}) and associated temperature anomalies (color scale; units: K) obtained by subtracting the mean value averaged in the storm-centered domain within a radius of 300 km: (a) RANK; (b) CTL. Bottom panels: inner-core radial profiles of (c) relative vorticity (units: 10^{-4} s^{-1}) and (d) tangential wind (units: m s^{-1}) near the surface layer.

1000 km. Initially, both cases have comparable Vmax (12.5 m s^{-1}) and RMW (150 km), but the inner-core radial profiles of relative vorticity are remarkably different (Figs. 1c and d). For the first vortex (named CTL hereafter), its maximum relative vorticity appears at the storm center and then decreases monotonically with the radius, indicating a negative radial gradient of relative vorticity (the so-called vortex β-effect). For the second one (named RANK), it is a classic Rankine-type vortex with a constant relative vorticity within the RMW. The initial tangential wind profiles vertically decrease as a sinusoidal function and vanish at 100 hPa. Once such tangential wind fields are specified, the mass and thermodynamic fields are obtained based on a nonlinear balance equation. Therefore, the initial vortex satisfies both hydrostatic and gradient wind balances. It is worth mentioning that the thermodynamical structures show some discrepancies as well. To satisfy the thermal wind balance, the decease of tangential wind with height requires a warm-core structure. In the current study, the maximum warm cores in both cases occur at the height of $z = 4$ km, albeit with different magnitudes. For instance, CTL has a slightly stronger warm core, implying this vortex has a lower central MSLP. In the following sections, we investigate how these inner-core differences affect the subsequent storm's evolution.

3. Numerical results

Figure 2 displays the evolution of intensities (represented by MSLP) in CTL and RANK, separately. In general, the vortices show little variations in intensity during the first 24 hours. Later on, both develop into a tropical storm after day 2, but with different intensification rates. Notice that CTL has a greater intensification rate compared with RANK. That is, starting from $t = 24$ h, the storm in CTL develops rapidly. The MSLP reaches about 970 hPa at $t = 48$ h of simulation, which is much lower than in RANK (~986 hPa) at the same time. To further demonstrate the discrepancies, the evolution of azimuthal-mean tangential winds at $z = 0.5$ km are plotted in Fig. 3. The results clearly show that, along with the enhanced tangential wind, the outer size increases but the RMW contracts. Nevertheless, the tangential wind reaches 40 m s^{-1} in CTL on day 2, which is about 10 m s^{-1} greater than in RANK. This indicates that small differences in the inner-core will result in significant variations in TC develop-

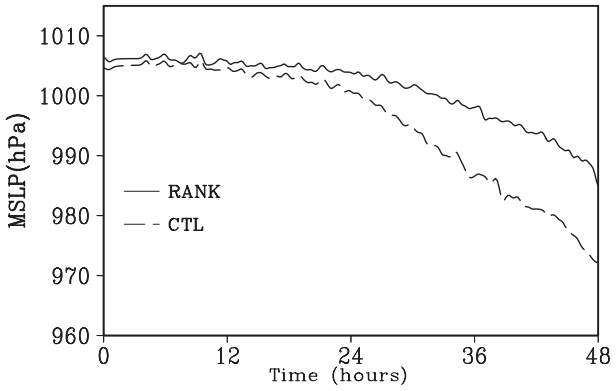

Fig. 2. Evolution of intensities (MSLP; units: hPa) in CTL and RANK.

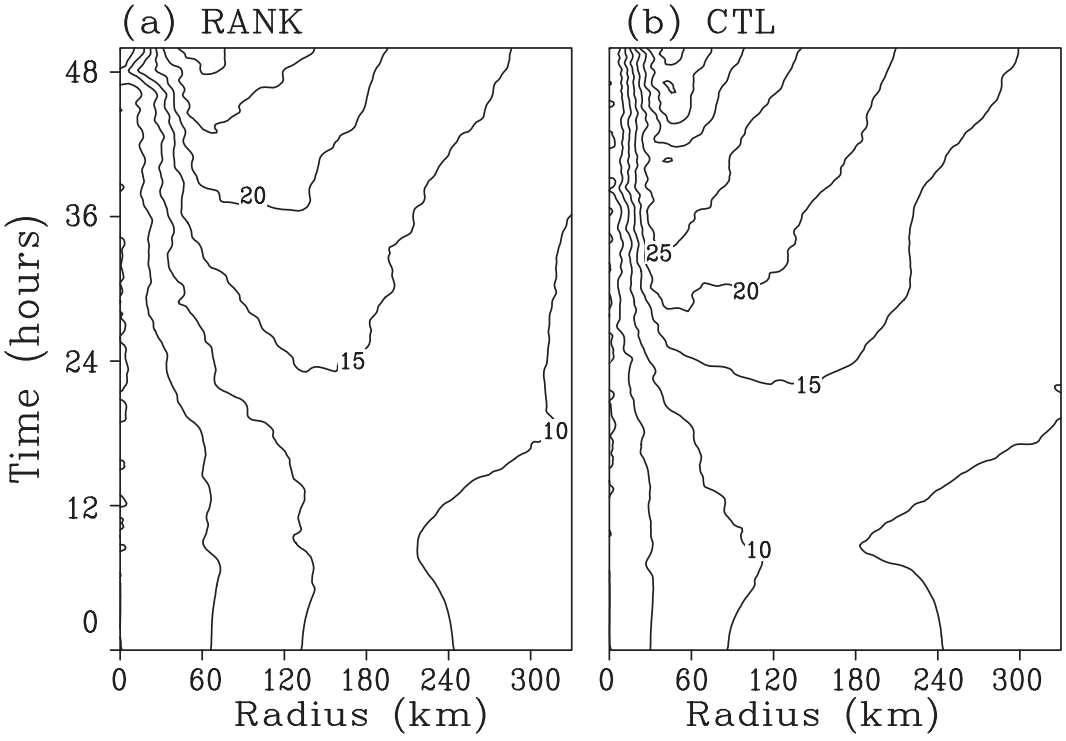

Fig. 3. Evolution of azimuthal-mean tangential wind (units: m s^{-1}) at $z = 0.5$ km in (a) RANK and (b) CTL.

ment.

Naturally, an interesting question arises: what is responsible for such discrepancies? Numerous studies (Hendricks et al., 2004; Montgomery et al., 2006; Houze et al., 2009) have pointed out that small-scale vortices, such as vortical hot towers (VHTs), play a prominent role in TC development. To reveal the roles of small-scale entities, we first examine the finer structure of the relative vorticity field. To this end, a spatial filtering (Ge et al., 2013b) is utilized to separate the small-scale convective cells from the system-scale or parent vortex. The variables will be separated into components with wavelength greater or less than 50 km, respectively. The component with wavelength less than 50 km approximately reflects the small-scale eddies, whilst the other represents the system-scale circulation. In this study, the terms of system-scale circulation and the parent vortex are interchangeable, and probably stand for the embryo of the storm. Fang and Zhang (2011) examined three scales ranging from the system-scale main vortex ($L > 150$ km) to the intermediate scale (50 km $< L <$ 150 km) and individual vorticity-rich convective cells ($L < 50$ km). Here, the separation only consists of two scales, and the choice of 50 km is somewhat arbitrary. Nevertheless, it will provide an opportunity to identify some salient features of system-scale and convective-scale circulation.

Figures 4 and 5 illustrate the evolution of relative vorticity at $z = 2$ km in RANK and CTL, respectively. The shaded area represents wavelength greater than 50 km and approximately reflects the system-scale circulation. The contours with wavelength shorter than 50 km denote the convective-scale vorticity anomalies (CVAs). In both cases, a large number of small-scale vorticity anomalies prevail around the genesis area, which agrees with previous numerical and observational studies (Hendricks et al., 2004; Houze et al., 2009; Ge et al., 2013a). Starting form $t = 12$ h, the CVAs emanate sporadically. With time, the CVAs spiral radially inward, merge frequently and eventually lead to a mesoscale system that will further evolve into the TC inner-core. This upscale cascade has been well demonstrated previously (Hendricks et al., 2004), and thus we only display some of the evolution characteristics of the CVAs. Obviously, there is a faster organization of CVAs in CTL, since the CVAs merge quickly into a well-organized structure at around $t = 24$ h. In RANK, although the CVAs rotate anticlockwise, the interactions, such as merge processes, are insignificant. For instance, the CVAs mainly circle around the center at a certain radius (i.e., 50 km), which is farther away from the center of the parent vortex compared to those in CTL. As a result, a poorly-organized inner-core structure can be identified during the period of interest.

In terms of the system-scale vorticity field, this probably represents the embryo of the storm. This circulation has a smooth and well-organized structure. Notice that the magnitude is larger in CTL compared with RANK. According to the so-called conditional instability of the second kind (Ooyama, 1964, 1982), a positive feedback exists between the boundary layer vorticity and the diabatic heating. The larger the boundary layer vorticity, the stronger the Ekman pumping and, thus, the greater the diabatic heating. Therefore, we speculate that a system-scale circulation with large vorticity is conducive to its own intensification. Furthermore, there are multi-scale interactions during the TC development process. These convective-scale eddies contribute to the sustainment and reinvigoration of moist convection, which in turn contributes to the maintenance and upscale growth of these vortices. On the one hand, the embedded small-scale CVAs will promote the system-scale circulation through the upscale growth; while on the other hand, the system-scale circulation provides a favorable environment for the CVAs.

Provided that there are salient differences in terms of the behavior (i.e., movements) of CVAs, it is helpful to address the following two questions: What is responsible for such different behavior of CVAs? And are the small-scale entities modulated by the system-scale one? For a typical TC-like vortex, the tangential wind peaks near the surface and decays upward, vertically. This indicates that there is vertical shear of the primary circulation and thus horizontal vorticity. Once the deep convection is triggered, each updraft will induce vorticity dipoles with negative and positive sign on either flank of the updraft, which is due to the tilting term in the vorticity tendency equation (Klemp, 1987). These vorticity dipoles will be split due to the vorticity segregation process (Schecter and Dubin, 1999; Van Sang et al., 2008). Specifically, small-scale cyclonic (anticyclonic) vorticity entities will move up (down) the ambient vorticity gradient. As a result, cyclonic vorticity anomalies tend to move toward the vortex center, while anticyclonic entities tend to move away from the center. As these positive vorticity eddies move radially inward and become closer to each other, they have a greater potential to merge together into a relatively larger-scale system. This process can be clearly demonstrated in a purely two-dimensional dynamics framework. In this study, the dry experiments are performed on a primitive equation model (Li et al., 2012). Figure 6 compares the different performances of vorticity eddies under different background vorticity gradients. Initially, four small-scale vorticity eddies are symmetrically embedded around the vortices. Interestingly, in CTL, with a negative vorticity gradient, these eddies rotate and rapidly distort to become strained out into filaments, which are eventually absorbed by the main vortex through axisymmetrization. In contrast, in the RANK-type case, the positive eddies rotate cyclonically along the initial radius and do not show radial inward movement. In other words, these entities are barely distorted by the refilamentation process, as in shown in CTL. These simple model results illustrate the important role of the background vorticity in modulating the embedded eddies.

Under complex circumstances, such as those in the TC inner area, Fang and Zhang (2011) investigated the evolution of negative vorticity anomalies and argued that the spiraling inward motion of these vorticity anomalies are mainly driven by the background flows. In this regard, the system-scale flow may modulate the behavior of individual convective anomalies. Hence, we speculate that, for a system-scale circulation with a stronger radial inflow, the conditions will promote the

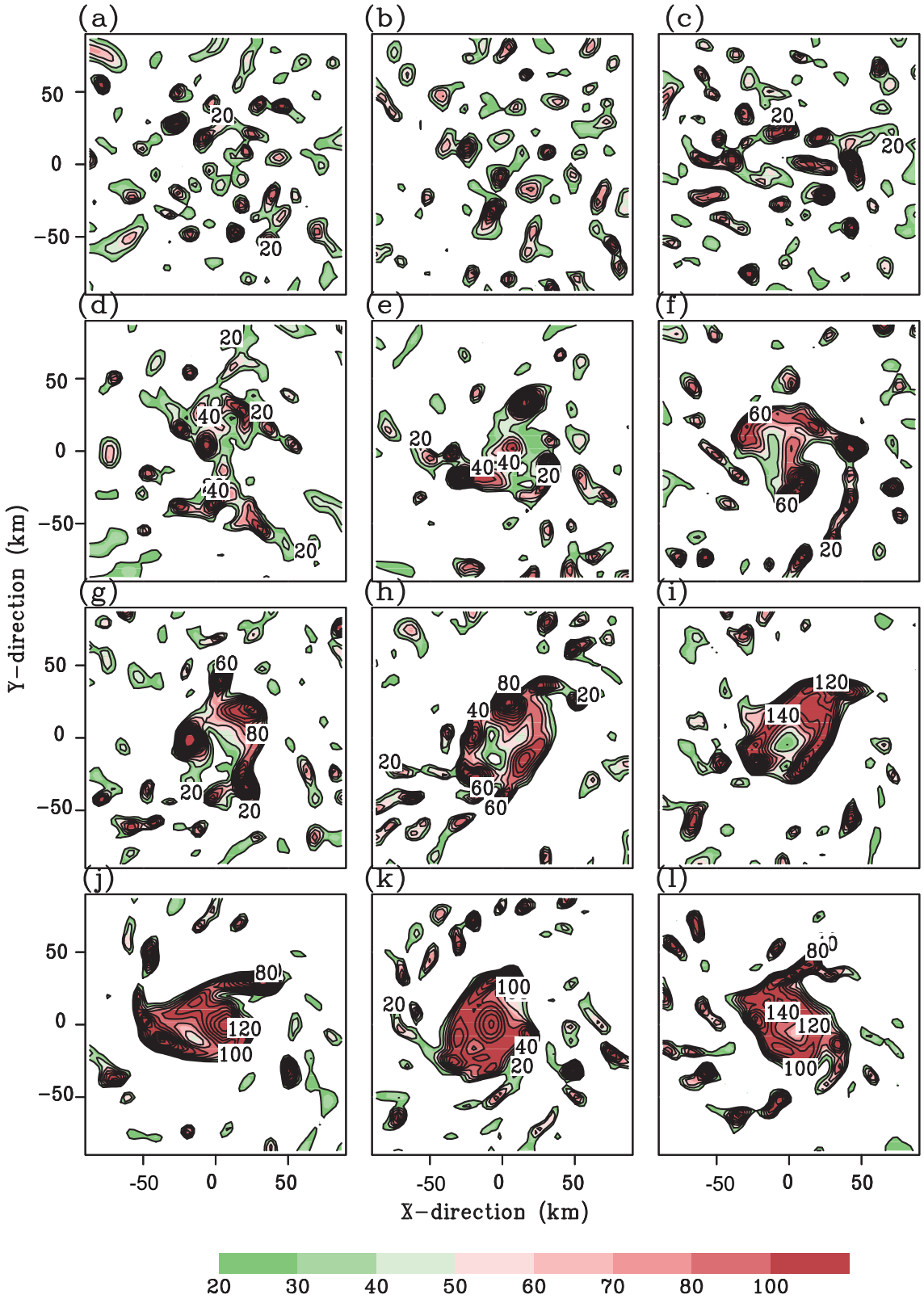

Fig. 4. Evolution of relative vorticity (units: 10^{-4} s^{-1}) at $z = 2$ km in CTL. The color scale (contours) denotes the system-scale (convective-scale) component. The panels (a–l) show the time period during $t = 12 - 34$ h, in 2-h intervals.

CVAs to move spirally inward. To this end, it is useful to compare the background (axisymmetric) flows. Figure 7 displays the vertical–radial profiles of azimuthal-mean tangential winds and radial flows in both cases. The boundary layer

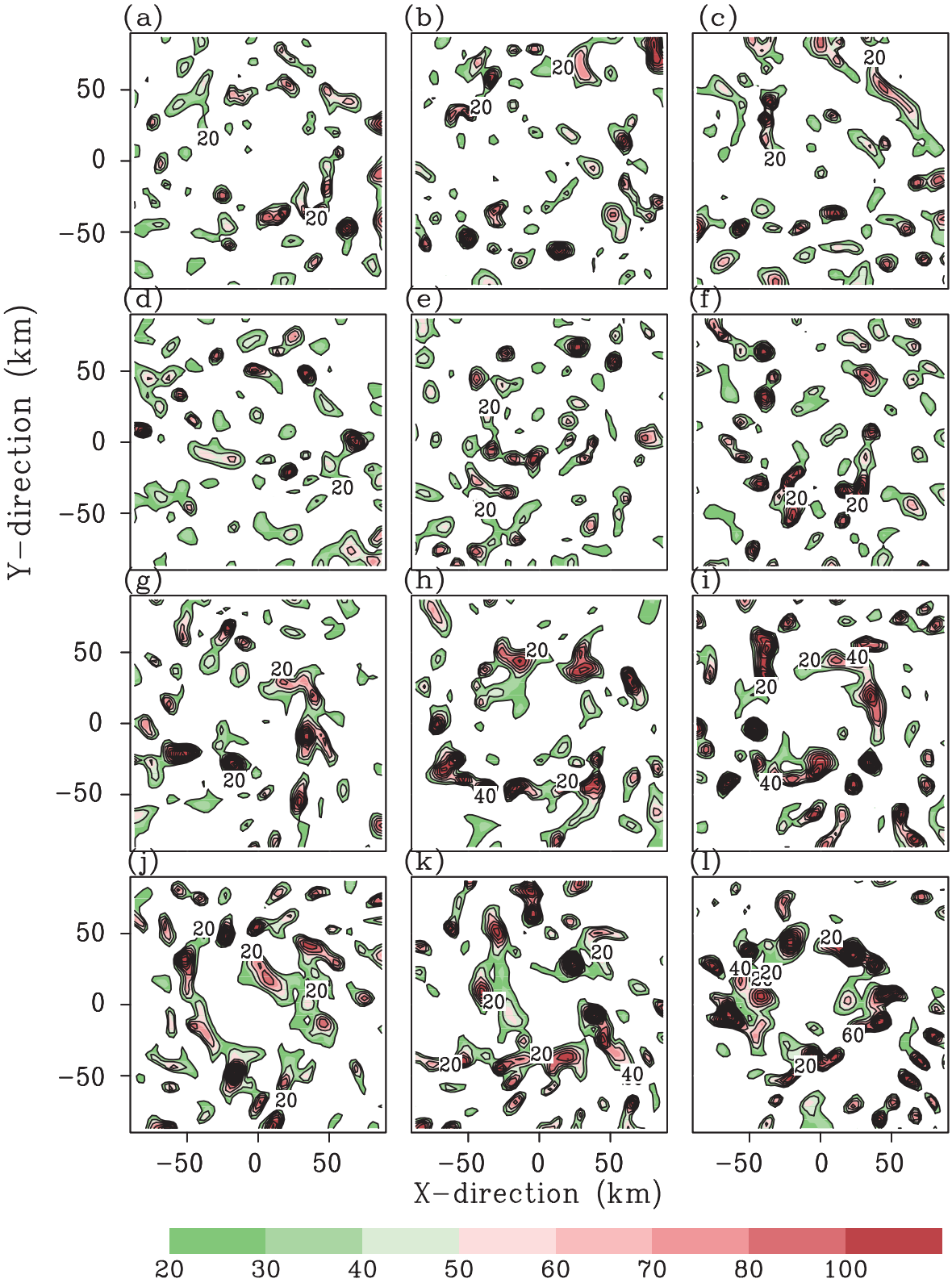

Fig. 5. As in Fig. 4 but for RANK.

inflows appear shortly after 12 hours of simulation, and enhance gradually with time. Meanwhile, the radial inflows extend inward. Notice that there are significant inflows in the inner area in CTL compared with RANK. Since the radial flow is initially set to zero in both experiments, the triggering of the radial flows lies in the breaking of a gradient wind balance due to surface friction. The greater the surface wind speed, the greater the friction and imbalance are. As shown in Fig.

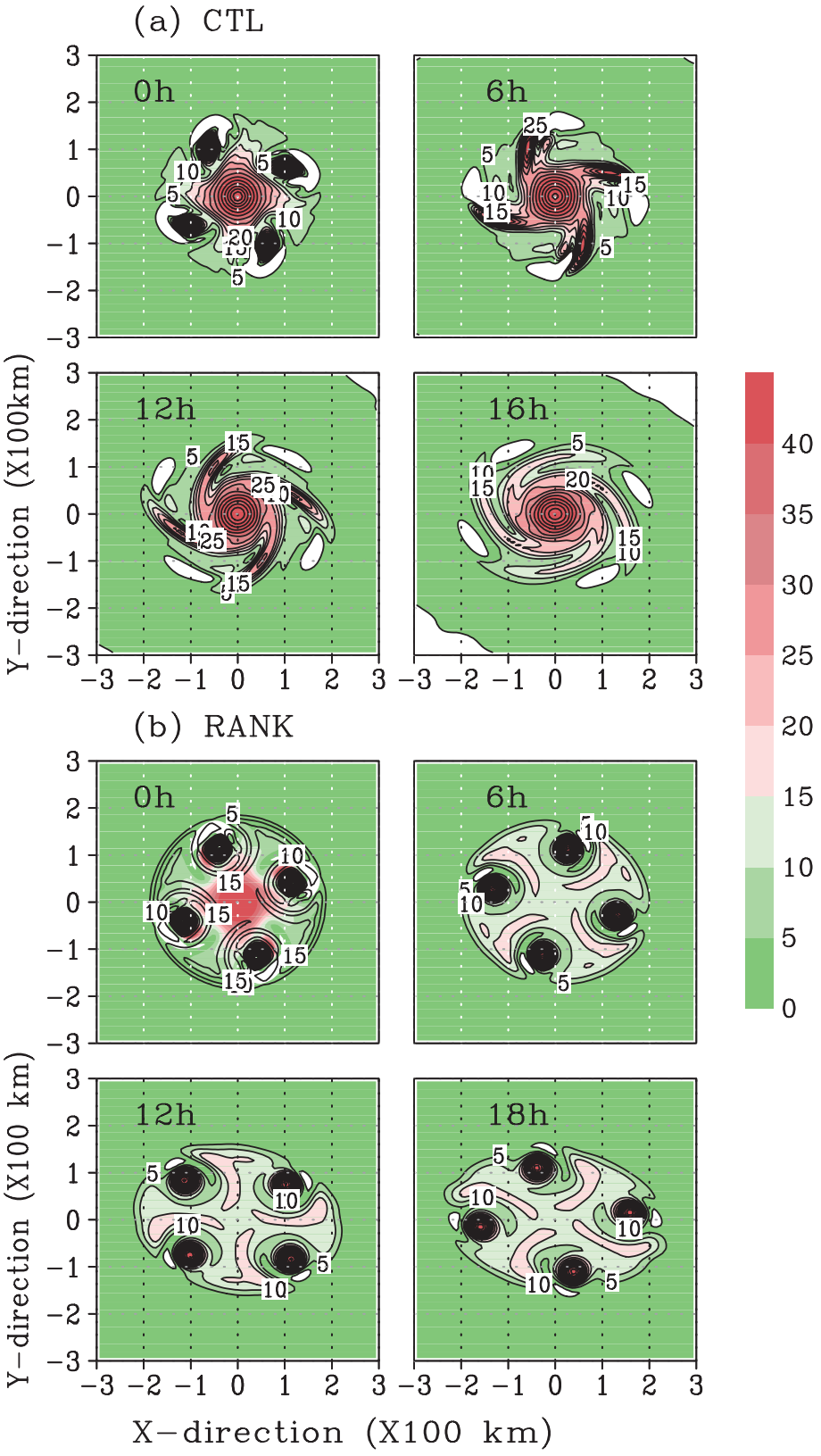

Fig. 6. Evolution of eddies under different background vorticity starting from $t = 0$ to 18 h, in time intervals of 6 h: (a) CTL; (b) RANK.

1, the wind speed in the inner area is slightly larger in CTL. In this regard, a greater imbalance will lead to a stronger radial inflow. To measure how differently the boundary layer gradient wind imbalance is excited under different vorticity

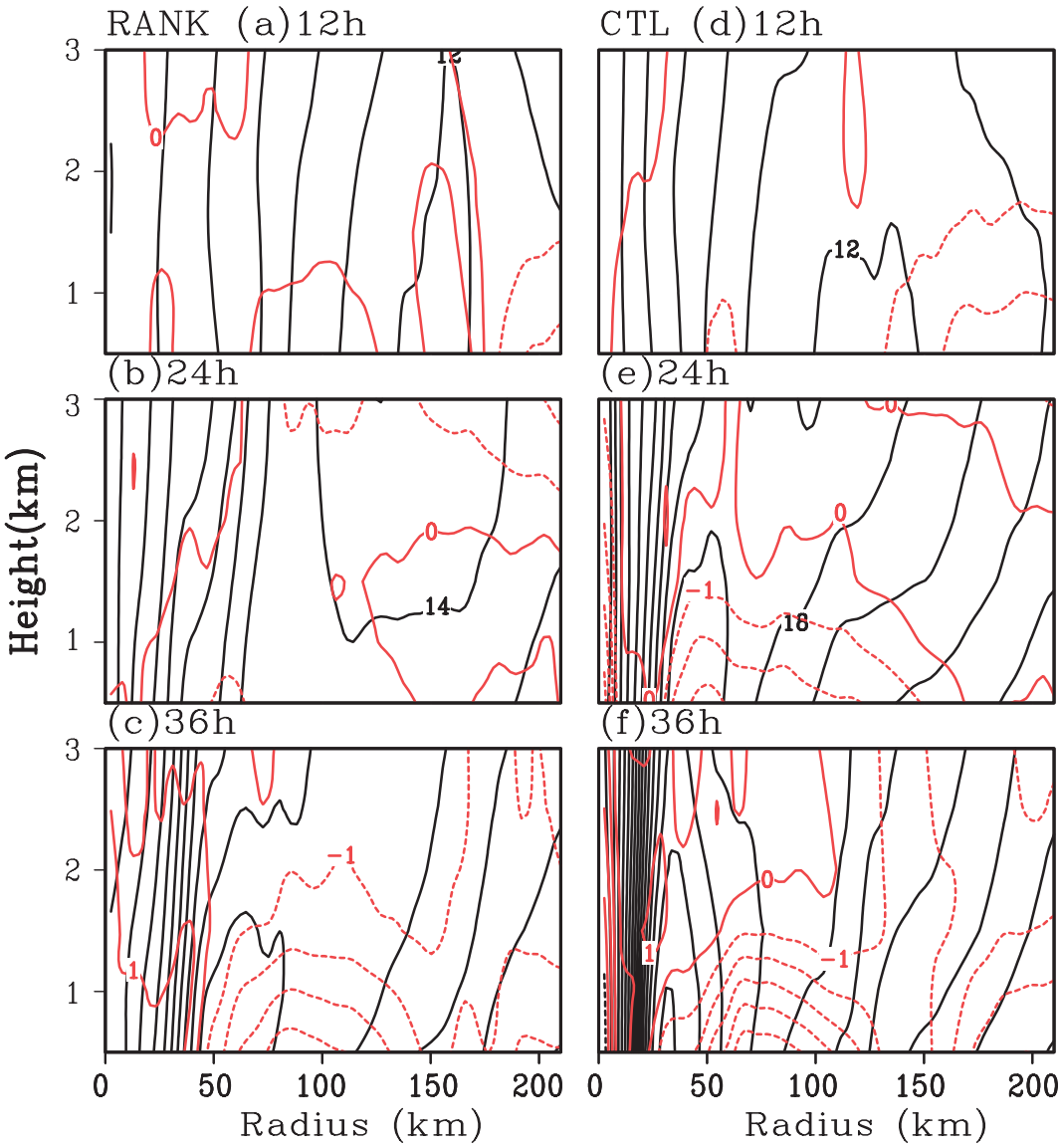

Fig. 7. Vertical–radial profiles of azimuthal-mean tangential winds (interval: 2 m s^{-1}; black solid lines) and radial flows (interval: 1 m s^{-1}; red lines): (a) RANK; (b) CTL.

conditions, we examine a net radial force field, following Li et al. (2012). The net radial force field is defined as the residual term of the gradient wind balance, reflecting a difference between the local radial pressure gradient and the sum of the centrifugal and Coriolis forces in the radial momentum equation, i.e.,

$$\mathrm{AF} = -\frac{1}{\rho}\frac{\partial \overline{P}}{\partial r} + f\overline{V} + \frac{\overline{V^2}}{r},$$

where P is the pressure, ρ is the air density, f is the Coriolis parameter, and V is the tangential wind. The overbar represents the azimuthal-mean component. If AF $= 0$, the tangential flow is in an exact gradient wind balance; if AF < 0, this flow is subgradient, indicating that there is a tendency to enhance the inflows toward the vortex center; and if AF > 0, it is supergradient, which means that there is a tendency to enhance the outflows away from the vortex center. Figure 8 shows the time–radius cross section of the azimuthal-mean net radial force field at $z = 500$ m. Note that in CTL the negative AF (i.e., subgradient flow) develops much earlier. It becomes evident at around 24 hours and continues to strengthen during the intensification period. In contrast, the negative inflow tendency is weaker in RANK. In short, it is likely that the difference in the radial wind between CTL and RANK can be primarily attributed to the extent to which the boundary layer imbalance is triggered.

Once the convection is triggered, the associated diabatic heating will drive the secondary circulation. Under the constraint of both the hydrostatic and gradient wind balance, the axisymmetric secondary circulation forced by the diabatic heating can be obtained through the Sawyer–Eliassen (SE) balance equation (Hendricks et al., 2004; Willoughby, 2009).

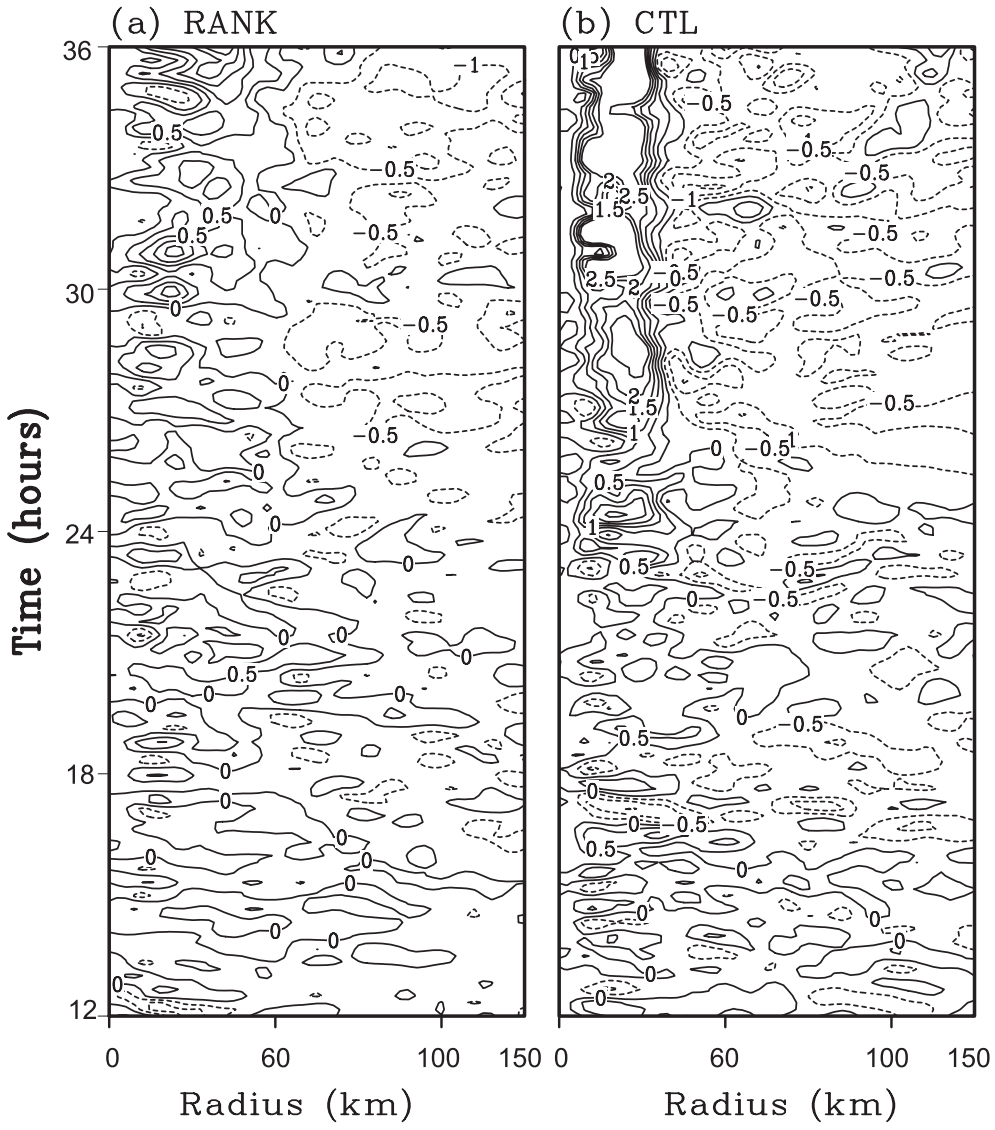

Fig. 8. Time–radial cross sections of gradient forcing (contours; units: 10^{-3} m s^{-2}): (a) RANK; (b) CTL.

This method is extensively used to diagnose the adjustment to reach a quasi-balanced state. For brevity, we do not introduce the details of the SE equation here. In this study, the azimuthal-mean diabatic heating forcing only is taken into account, since the spin-up of the system-scale secondary circulation is primarily ascribed to this term (Montgomery et al., 2006; Nolan, 2007). Figure 9 compares the components (i.e., the radial inflow and vertical motion) in the model simulations and forced by the SE equation, separately. The model simulation clearly shows the azimuthal-mean lower-level inflow and upper-level outflow. This basic structure is successfully obtained through the SE method, although the strength is comparatively weaker than in the model simulation. The main differences exist in the boundary layer and upper outflow layer, where the balance assumptions are not fully satisfied (Smith and Montgomery, 2008). Admittedly, some discrepancies may come from other forcing terms such as the momentum forcing and frictional effect, which are neglected here. Nevertheless, the results suggest that the diabatic heating does indeed play a vital role in vortex spin-up. The mean radial circulation in CTL is considerably stronger than in RANK during the period of interest (i.e., averaged during 24–36 h). Around the TC genesis area, the strong diabatic heating is generated by the convective VHTs. Once the convection is triggered, the diabatic heating will be released, and then converted into kinetic energy through the balance adjustment. It is apparent that the genesis efficiency (i.e., the conversion ratio of the diabatic heating to the kinetic energy) is largely proportional to the inertial parameter. Under the condition that the inertial stability is larger, the efficiency is higher (Schubert and Hack, 1982; Hack and Schubert, 1986). Physically, a larger inertial stability corresponds to a smaller Rossby deformation radius. With a smaller Rossby deformation radius, the energy produced by the diabatic heating is likely confined within a smaller radius, rather than dispersed by gravity waves. Accordingly, there is a consider-

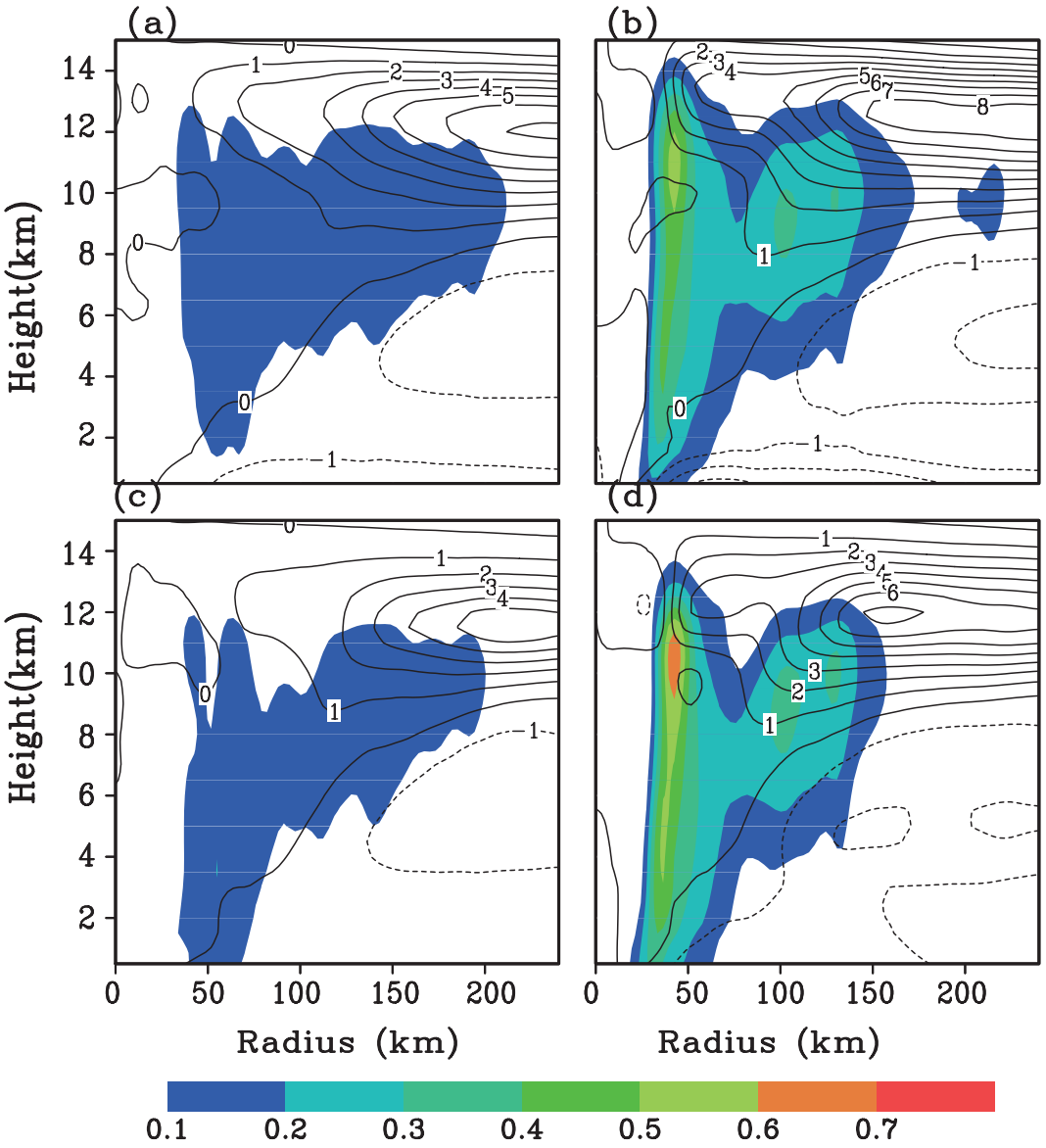

Fig. 9. Radial inflow (contours; units: m s^{-1}) and vertical motion (color scale; units: m s^{-1}) averaged during $t = 24 - 36$ h. Panels (a, b) are the model simulations for RANK and CTL, respectively; panels (c, d) are derived from the SE equation for RANK and CTL, respectively.

able balance response of the system-scale vortex to the heating forcing, and the system-scale secondary circulation will be greatly enhanced. The strong convergent lower-level inflow helps the storm to spin up through the convergence of absolute angular momentum. In turn, the convergent inflow encourages the CVAs to move inward. This will help interactions, such as merger interactions, and lead to a single but more intense vorticity anomaly. Thereafter, the so-called system-scale intensification mechanism will become important (Tory et al., 2006).

Figure 10 shows that the radius–height cross section of symmetric components of the diabatic heating and inertial stability, $I^2 = (f+\zeta)(f+2V/r)$, averaged during $t = 24-36$ h. Here ζ is the relative vorticity. Consistent with the rapid intensification in CTL, the inertial stability and diabatic heating are much greater than those in RANK. Meanwhile, the radial location of the maximum diabatic heating is closer to the storm center in CTL. As revealed by Rogers et al. (2013), one of the key inner-core structural differences between intensifying and steady-state TCs is the radial location of convective bursts. For intensifying cases, the convective bursts are situated closer to the storm center. Our results support their findings. In short, both the vorticity segregation process and system-scale inflow likely explain the different intensification rates. This upscale cascade is considered as the first key step toward cyclogenesis. On the one hand, the CVAs provide seed vorticity that contributes to the vortex upscale cascade; while on the other hand, the net heating from these convective updrafts drives the transverse circulation necessary for the spin up of the azimuthal-mean vortex.

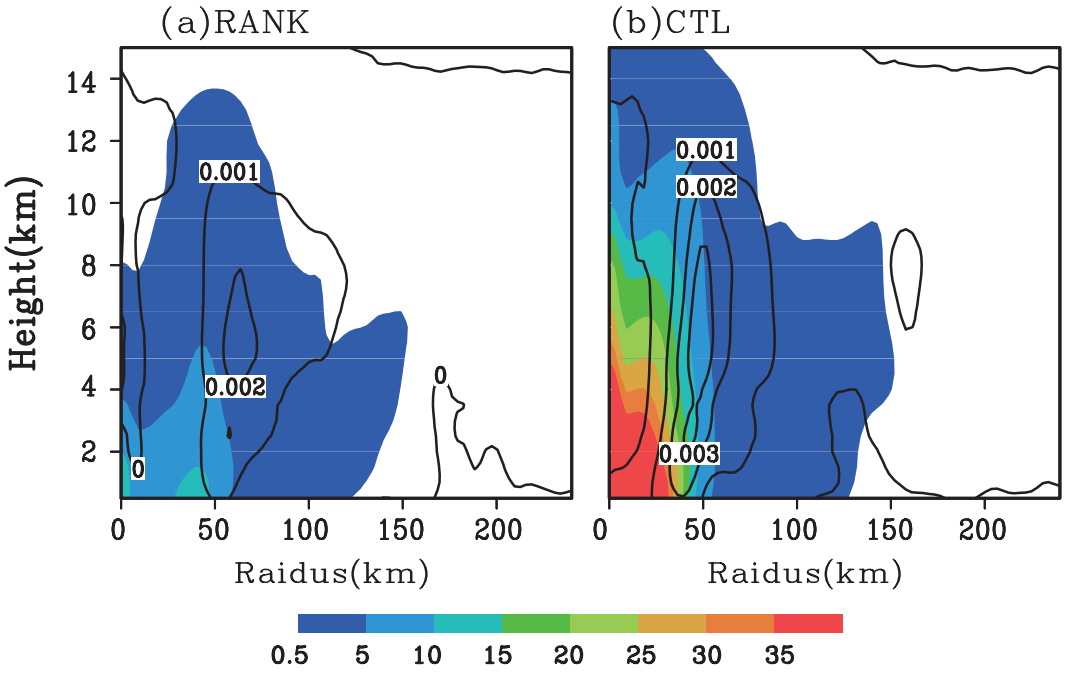

Fig. 10. Averaged radius–height cross section of symmetric components of diabatic heating (contours; units: K s^{-1}) and inertial stability I^2 (color scale; units: 1×10^{-7} s^{-2}) during $t = 24 - 36$ h.

4. Summary and discussion

The dependence of TC development on the initial structure of the parent vortex is explored using a set of idealized numerical simulations. It is found that the ability of the parent vortex to maintain itself and intensify further into an incipient TC can depend strongly on its structure. For a system with a larger inner-core vorticity/inertial stability, the conversion ratio of the diabatic heating to kinetic energy is greater. Furthermore, the behavior of the convective vorticity eddies is likely modulated by the system-scale circulation. Both vorticity segregation and system-scale circulation affect the upscale growth of the convective vorticity eddies. Generally, the larger the background vorticity, the greater the Ekman pumping, and the more prolific the convection. A parent vortex with a larger relative vorticity will promote CVA formation, radial propagation and, thus, a greater potential for merger. In turn, the diabatic heating closer to the storm center, along with higher inertial stability, will efficiently enhance the system-scale secondary circulation.

The results presented here also suggest that an important issue is to include structural parameters in operational forecasts. By this reasoning, more work is needed to validate initial and forecasted storm structures. Hopefully, with sufficient observations, such as those from airborne dual Doppler radar data, advanced data assimilation methods such as 4DVAR and EnKF can correctly initialize TCs (Xiao et al., 2000; Wu et al., 2006; Zhang et al., 2011). Furthermore, when we monitor TC genesis, it is important to compare the radial structure instead of simply comparing with parameters such as Vmax and MSLP only. Since small-scale vortices are typically formed within clusters of cumulonimbi, a structural comparison might offer some predictive insight into which cloud clusters have a better chance of undergoing tropical cyclogenesis. Finally, in the current study, only highly idealized vortices with weak strength are examined. More cases with different intensities should be examined in order to reveal the impacts of initial inner-core structure on TC rapid intensification.

Acknowledgements. The authors thank Dr. WU Liguang for his comments. This work was jointly sponsored by the National Key Basic Research Program of China (Grant No. 2015CB452803), the State Key Laboratory of Severe Weather, Chinese Academy of Meteorological Sciences (Grant No. 2014LASW-B08), the "six peaks of high-level talents" funding project, and the Key University Science Research Project of Jiangsu Province (Grant No. 14KJA170005).

REFERENCES

Elsberry, R. L., 2005: Achievement of USWRP hurricane landfall research goal. *Bull. Amer. Meteor. Soc.*, **86**, doi: 10.1175/BAMS-86-5-643.

Fang, J., and F. Q. Zhang, 2011: Evolution of multiscale vortices in the development of Hurricane Dolly (2008). *J. Atmos. Sci.*, **68**, 103–122.

Ge, X. Y., T. Li, and M. S. Peng, 2013a: Tropical cyclone genesis efficiency: Mid-level versus bottom vortex. *J. Trop. Meteor.*, **19**, 197–213.

Ge, X. Y., T. Li, and M. Peng, 2013b: Effects of vertical shears and midlevel dry air on tropical cyclone developments. *J. Atmos. Sci.*, **70**, 3859–3875.

Hack, J. J., and W. H. Schubert, 1986: Nonlinear response of atmospheric vortices to heating by organized cumulus convection.

J. Atmos. Sci., **43**, 1559–1573.

Hendricks, E. A., M. T. Montgomery, and C. A. Davis, 2004: The role of "vortical" hot towers in the formation of Tropical Cyclone Diana (1984). *J. Atmos. Sci.*, **61**, 1209–1232.

Hendricks, E. A., M. S. Peng, X. Ge, and T. Li, 2011: Performance of a dynamic initialization scheme in the coupled ocean-atmosphere mesoscale prediction system for tropical cyclones (COAMPS-TC). *Wea. Forecasting*, **26**, 650–663.

Houze Jr., R. A., W.-C. Lee, and M. M. Bell, 2009: Convective contribution to the genesis of Hurricane Ophelia (2005). *Mon. Wea. Rev.*, **137**, 2778–2800.

Jordan, C. L., 1958: Mean soundings for the West Indies area. *J. Meteor. Sci.*, **15**, 91–97.

Klemp, J. B., 1987: Dynamics of tornadic thunderstorms. *Annu. Rev. Fluid Mech.*, **19**, 369–402.

Kurihara, Y., M. A. Bender, and R. J. Ross, 1993: An initialization scheme of hurricane models by vortex specification. *Mon. Wea. Rev.*, **121**, 2030–2045.

Leslie, L. M. and G. J. Holland, 1995: On the bogussing of tropical cyclones in numerical models: A comparison of vortex profiles. *Meteor. Atmos. Phys.*, **56**, 101–110.

Li, T., X. Y. Ge, M. Peng, and W. Wang, 2012: Dependence of tropical cyclone intensification on the Coriolis parameter. *Tropical Cyclone Research and Review*, **1**, 242–253.

Liang, J., L. G. Wu, and H. J. Zhong, 2014: Idealized numerical simulations of tropical cyclone formation associated with monsoon gyres. *Adv. Atmos. Sci.*, **31**, 305–315, doi: 10.1007/s00376-013-2282-1.

Lin, Y.-L., R. D. Rarley, and H. D. Orville, 1983: Bulk parameterization of the snow field in a cloud model. *J. Climate Appl. Meteor.*, **22**, 1065–1092.

Liu, Q., S. Lord, N. Surgi, Y. Zhu, R. Wobus, Z. Toth, and T. Marchok, 2006: Hurricane relocation in global ensemble forecast system. *Preprints*, 27*th Conference on Hurricanes and Tropical Meteorology*, Monterey, CA, Amer. Meteor. Soc., P5. 13.

Montgomery, M. T., M. E. Nicholls, T. A. Cram, and A. B. Saunders, 2006: A vortical hot tower route to tropical cyclogenesis. *J. Atmos. Sci.*, **63**, 355–386.

Nolan, D. S., 2007: What is the trigger for tropical cyclogenesis? *Aust. Meteor. Mag.*, **56**, 241–266.

Ooyama, K., 1964: A dynamical model for the study of tropical cyclone development. *Geofis. Int.*, **4**, 187–198.

Ooyama, K. V., 1982: Conceptual evolution of the theory and modeling of the tropical cyclone. *J. Meteor. Soc. Japan*, **60**, 369–370.

Rogers, R., P. Reasor, and S. Lorsolo, 2013: Airborne Doppler observations of the inner-core structural differences between intensifying and steady-state tropical cyclones. *Mon. Wea. Rev.*, **141**, 2970–2991.

Schecter, D. A., and D. H. E. Dubin, 1999: Vortex motion driven by a background vorticity gradient. *Phys. Rev. Lett.*, **83**, 2191–2194.

Schubert, W. H., and J. J. Hack, 1982: Inertial stability and tropical cyclone development. *J. Atmos. Sci.*, **39**, 1687–1697.

Smith, R. K, and M. T. Montgomery, 2008: Balanced boundary layers used in hurricane models. *Quart. J. Roy. Meteor. Soc.*, **134**, 1385–1395.

Tory, K. J., M. T. Montgomery, and N. E. Davidson, 2006: Prediction and diagnosis of tropical cyclone formation in an NWP system. Part I: The critical role of vortex enhancement in deep convection. *J. Atmos. Sci.*, **63**, 3077–3090.

Van Sang, N., R. K. Smith, and M. T. Montgomery, 2008: Tropical-cyclone intensification and predictability in three dimensions. *Quart. J. Roy. Meteor. Soc.*, **134**, 563–582.

Wang, B., and X. Zhou, 2008: Climate variation and prediction of rapid intensification in tropical cyclones in the western North Pacific. *Meteor. Atmos. Phys.*, **99**, 1–16.

Willoughby, H. E., 2009: Diabatically induced secondary flows in tropical cyclones. Part II: Periodic forcing. *Mon. Wea. Rev.*, **137**, 822–835.

Willoughby, H. E., and P. G. Black, 1996: Hurricane Andrew in Florida: Dynamics of a disaster. *Bull. Amer. Meteor. Soc.*, **77**, 543–549.

Wu, C.-C., K.-H. Chou, Y. Q. Wang, and Y.-H. Kuo, 2006: Tropical cyclone initialization and prediction based on four-dimensional variational data assimilation. *J. Atmos. Sci.*, **63**, 2383–2395.

Wu, L. G., J. Liang, and C.-C. Wu, 2011: Monsoonal influence on Typhoon Morakot (2009). Part I: Observational analysis. *J. Atmos. Sci.*, **68**, 2208–2221.

Xiao, Q. N., X. L. Zou, and B. Wang, 2000: Initialization and simulation of a landfalling hurricane using a variational bogus data assimilation scheme. *Mon. Wea. Rev.*, **128**, 2252–2269.

Xu, J., and Y. Q. Wang, 2010: Sensitivity of tropical cyclone inner-core size and intensity to the radial distribution of surface entropy flux. *J. Atmos. Sci.*, **67**, 1831–1852.

Zhang, F. Q., Y. H. Weng, J. F. Gamache, and F. D. Marks, 2011: Performance of convection-permitting hurricane initialization and prediction during 2008–2010 with ensemble data assimilation of inner-core airborne Doppler radar observations. *Geophy. Res. Lett.*, **38**, L15810, doi: 10.1029/2011GL048469.